CFD humidity and temperature modelling in the ATLAS ITK Strip

TP Mafa[2], M. Bhamjee[1], S.H. Connell[1], L.L. Leeuw[3]

[1]University of Johannesburg
[2]University of South Africa
[3]University of the Western Cape

SAIP 2022, 1-8 July 2022

Outline

- Introduction
- The mathematical (CFD) model
- CFD geometry and boundary conditions
- Numerical results
- Conclusion

Introduction

- The ATLAS Detector [1, 2] at the Large Hadron Collider at CERN is engaged in an Upgrade Process which is expected to be ready for installation and commissioning in 2024.
- This "Phase II" upgrade [3] will implement radical performance improvements to the ATLAS detector to prepare it for new era of the High Luminosity LHC (or HL-LHC).
- The part of the detector which tracks particles, the Inner Tracker (ITk), will be rebuilt to allow more precise tracking at higher rates while withstanding the harsh radiation environment.

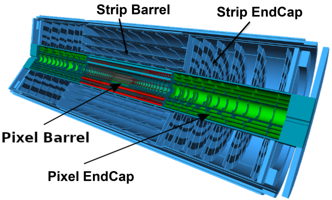

FIGURE – 0 : ATLAS ITK

Introduction

- The aim of this work is to understand the humidity and temperature environment in the ITK strip region, in particular to study the dead spaces of low atmosphere renewal rates and the propagation of vapour from leak events, under various planned and failure conditions. The humidity monitoring via dew point measurements will prevent condensation of moisture where this can cause harm.
- We use the Computational Fluid Dynamics (CFD) simulation with ANSYS Fluent [6] to describe the simplified model of ITK, which has a lowered detail in the geometry and materials, while keeping in place the major elements responsible for accurate physics performance.

Mathematical (CFD) model

The CFD flow solver based on finite volume method is used in the present work to solve Reynolds-averaged Navier-Stokes (RANS) and species transport equations

Continuity and momentum equations

$$\frac{\partial \rho}{\partial t} + \frac{\partial(\rho u_i)}{\partial x_i} = 0, \tag{1}$$

$$\frac{\partial(\rho u_i)}{\partial t} + \frac{\partial(\rho u_i u_j)}{\partial x_j} = -\frac{\partial p}{\partial x_j} + \mu \frac{\partial^2 u_i}{\partial x_j \partial x_j} - \frac{\partial(\rho \overline{u'_i u'_j})}{\partial x_j} - \rho g_j, \tag{2}$$

the indices i and j take the values 1,2,3. The parameters u_i is the average velocity, $\overline{u'}_i$ is the fluctuation velocity, ρ is the fluid density and $\mu = \mu_s + \mu_t$ is the viscosity coefficient. The coefficient μ_s is the molecular viscosity (kg/ms) and μ_t is the turbulent viscosity, defined as $\mu_t = \rho C_\mu \frac{k^2}{\varepsilon}$. The term $-\rho\overline{u'_i u'_j} = \tau_{ij}$ is the Reynolds stress tensor

Mathematical (CFD) model

For standard k-ε model, the transport equations for the turbulent kinetic energy and the dissipation rate are given by :

The transport and dissipation rate equations

$$\frac{\partial(\rho k)}{\partial t} + u_j \frac{\partial(\rho k)}{\partial x_j} = \frac{\partial}{\partial x_j}\left[\left(\mu + \frac{\mu_t}{\sigma_k}\right)\frac{\partial k}{\partial x_j}\right] - \rho\varepsilon + \tau_{ij}\frac{\partial u_i}{\partial x_j}, \tag{3}$$

$$\begin{aligned}\frac{\partial(\rho\varepsilon)}{\partial t} + u_j \frac{\partial(\rho\varepsilon)}{\partial x_j} &= \frac{\partial}{\partial x_j}\left[\left(\mu + \frac{\mu_t}{\sigma_\varepsilon}\right)\frac{\partial \varepsilon}{\partial x_j}\right] \\ &\quad - c_{\varepsilon 1}\frac{\varepsilon}{k}\tau_{ij}\frac{\partial u_i}{\partial x_j} - c_{\varepsilon 2}\rho\frac{\varepsilon^2}{k}.\end{aligned} \tag{4}$$

where k is the turbulent kinetic energy. k measure how much energy is contained in the fluctuation. ε is the turbulent dissipation. ε measure the rate at which turbulent kinetic energy is dissipated.

Mathematical (CFD) model

The Turbulent k-ε use the Boussinesq hypothesis to link the Reynolds stress tensor τ_{ij} to the mean velocity gradients as follows

$$\tau_{ij} = -\rho\overline{u_i'u_j'} = \mu_t\left(\frac{\partial u_i}{\partial_j} + \frac{\partial u_j}{\partial_i}\right) - \frac{2}{3}\left(\rho k + \mu_t\frac{\partial u_k}{\partial_k}\right)\delta_{ij}. \tag{5}$$

The heat transfer equation for energy conservation

$$\begin{aligned}\frac{\partial(\rho E)}{\partial t} &= -u_j\frac{\partial(\rho E)}{\partial x_j} - p\frac{\partial u_j}{\partial x_j} + k_t\frac{\partial^2 T}{\partial x_j \partial x_j} \\ &\quad +\tau_{ij}\frac{\partial u_i}{\partial x_j} - \frac{\partial}{\partial x_j}\left(\sum_j^n m_j h_j\right) + S_j, \end{aligned} \tag{6}$$

where k_t is the thermal conductivity, T is temperature, E is the energy and S_j is the source energy.

Mathematical (CFD) model

Conservation equations describing convection, diffusion, and reaction sources for each component species.

$$\frac{\partial}{\partial t}(\rho Y_i) + \frac{\partial(\rho u_j Y_i)}{\partial x_j} = -\frac{\partial J_i}{\partial x_j} + R_i + S_{Y_i}, \tag{7}$$

$$J_i = \left(\rho D_{i,m} + \frac{\mu_t}{S_{C_t}}\right)\frac{\partial Y_i}{\partial x_j}, \tag{8}$$

where Y_i, the local mass fraction of each species, R_i is the net rate of production of species i by chemical reaction and S_i is the rate of creation by addition from the dispersed phase plus any user-defined sources, J_i is the diffusion flux of species i, which arises due to concentration gradients. $D_{i,m}$ is the diffusion coefficient for species, i, in the mixture, and S_{c_t} is the turbulent Schmidt number

CFD geometry and boundary conditions

We started with the simplified ITK volume represented in Figure 1. The geometry does not include the petals and staves.

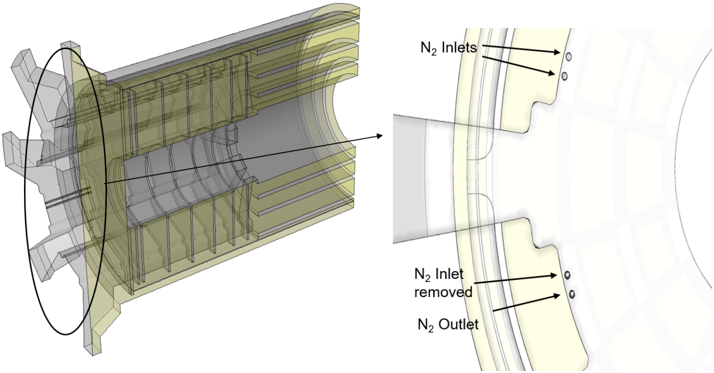

FIGURE – 1 :The N_2 gas flushing concepts of Strip Endcap and Barrel

CFD geometry and boundary conditions

CFD model geometry displaying the quarter of the ITK Strip. Both quarter designs dispose two inlets, one outlet and three leaks, which means the full ITK geometry has a total of eight inlets, four outlets and twelve leaks

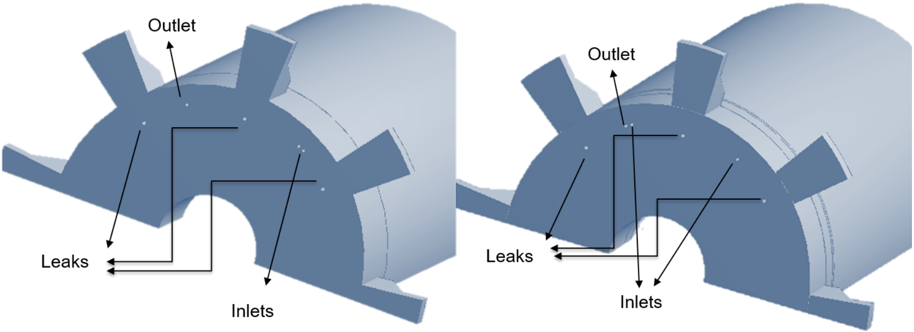

FIGURE – 2 : Old piping position is shown on the left and new piping position on the right.

CFD geometry and boundary conditions

Model input and boundary conditions

1. Inlets, Outlet and Leaks:

Boundary	Type	Mass Flow/ Velocity	Temp (ºC)	Species	Humidity
Inlets (2 manifolds)	Uniform Velocity Inlet	2.4 m/s (per inlet tube)	15	N_2	0%
Outlet	Pressure Outlet	Atmospheric Pressure	Fluent Calculated	Mixture – Fluent Calculated	Fluent Calculated
Leaks	Mass Flow Inlet	0,0083333l/s per leak (12 leaks total)	25	Air (composition - nitrogen (mass fraction of 0.78), oxygen (mass fraction of 0.21), water vapour (mass fraction of 0.01).)	50-60%

2. Walls:

Boundary	Type	Heat Transfer Conditions	Temp (ºC)	Material
OSV Outer Wall	Wall	Constant Temperature	10	Graphite
Detector Disks	Wall	Constant Temperature	-25	Graphite
Rest	Wall	Coupled	Fluent Calculated	Polymoderator and Skin – Glass-plate Inlet and outlet tubes - PEEK

FIGURE – 3 : Model input and boundary conditions.

Numerical results

The effect of the S-bend on the nitrogen N_2 inlets velocity [m/s]

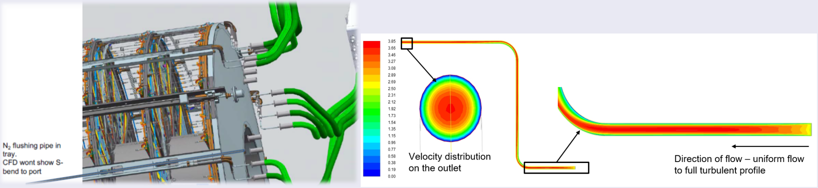

FIGURE – 4 : Modelled S-bend for the N_2 flushing pipe.

- Development of full turbulence profile is observed and the average velocity don't change from S-bend inlet to the outlet.
- The area weighted average velocity on outlet is 2.4 m/s ; thus there is no need to include this profile in the ITK simulation.

Numerical results

The velocity pathlines [m/s] from inlets and outlet.

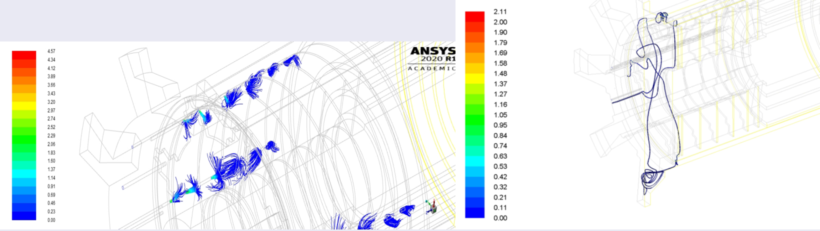

FIGURE – 5 : Model input and boundary conditions

- The figure on the left displays a non uniform distribution of nitrogen (N_2) via jets manifold. Common problem with distributed manifolds.
- The Figure on the right shows that there is no short-circuit from inlet to outlet. Thus, the outlet position in Figure - 2 is not an issue.

Numerical results

The temperature and humidity profiles of the ITK model with leaks for the old piping position

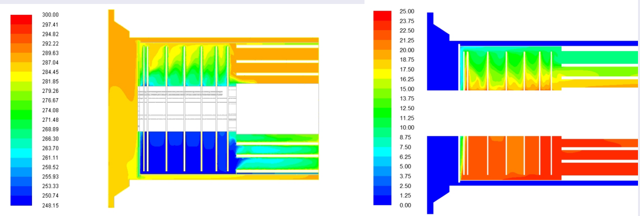

FIGURE – 6 : Temperature and Relative humidity profiles.

- Non uniform circulation of the flow.
- Higher temperature up and lower temperature below with a sharp humidity gradient.
- The necessity of moving one inlet pipe close to the outlet was required

Numerical results

The temperature and humidity profiles of the ITK model with leaks for the new piping position

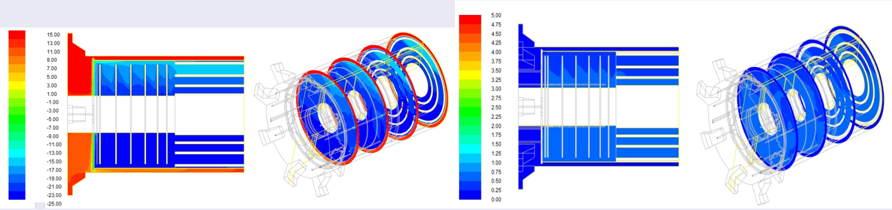

FIGURE – 7 : Temperature in XZ plane as well numerous location along Z at the inleak rate of 0.02l/s.

- Sufficiently low humidity in the OSV as required and expected. For the leak rate of 0.02l/s, we noticed a significant low relative humidity throughout the ITK volume
- More uniform temperature distribution than in the old piping position

Numerical results

The dew point was calculated by implementing the Bögel modification of the Magnus formula

Formula for the dew point

$$\gamma_m(T, R_h) = \ln\left(\frac{R_H}{100} e^{\left(b-\frac{T}{d}\right)\left(\frac{T}{c-T}\right)}\right) \tag{9}$$

$$T_{d_p} = \frac{c\gamma_m(T, R_h)}{b - \gamma_m(T, R_h)}, \tag{10}$$

where the constants $a = 6.1121$ mbar, $b = 18678$ mbar, $c = 257.14\ ^\circ C$, $d = 234.5\ ^\circ C$.

Numerical results

The dew point profile for the ITK model with leaks

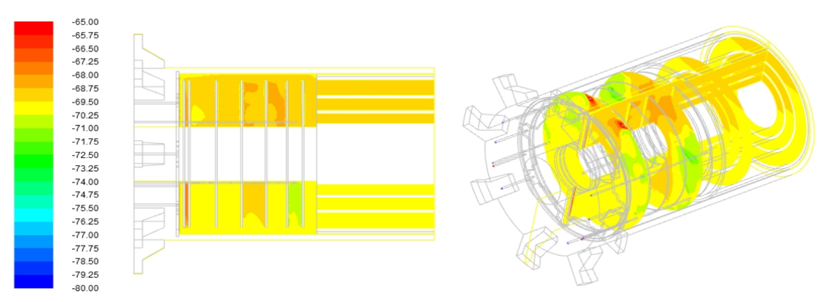

FIGURE – 8 : Temperature in XZ plane as well numerous location along Z at the inleak rate of 0.02 l/s

- dew point also varies significantly closer to the stiffener disc. Also notable variation higher up. Volume Average is - 69.70 $^\circ C$ in the Strip Endcap and Barrel region.

Conclusion

- The results showed that there is no risk of short-circuit in piping design from inlets to outlets.
- The findings also displayed a non uniform distribution with attenuation along the length and this feature led to the new manifold design proposition.
- The model revealed a lower temperature and high relative humidity at the bottom of Strip Endcap and Barrel.
- This feature can be justified by high velocity at the top and low velocity at the bottom, driven by convection and buoyancy effect, allowing enough time for moisture to accumulate.

Conclusion

- It noticed also a very low flow supply in the region of Strip Barrel. This problem is due to the use of solid disks rather then interleaved petal structure, forcing the flow to pass only between the detector walls and the OSV region.
- Based on the model settings, we provide an initial estimate of the maximum permissible inleak rate to keep the dew point below -60$^{\circ}C$ in the Strip Endcap and Barrel regions .
- The findings indicate that at the specified inleak rate and Nitrogen flushing rate, ATLAS ITK will obtain a specified dryness. These findings were confirmed in our similar study, by including petals and staves in the Strip Endcap and Barrel.

References

1. ATLAS Collaboration, The ATLAS Experiment at the CERN Large Hadron Collider, JINST 3 (2008) 235 S08003 (cit. on p. 2).
2. ATLAS : A 25-Year Insider Story of the LHC Experiment, World Scientific, 2019, isbn : 978-981-327- 237 179-1 (cit. on p. 2).
3. The ATLAS Collaboration, ATLAS Letter of Intent Phase-I Upgrade, CERN-2011-012 (2011) (cit. on 239 p. 2).
4. The ATLAS Collaboration, Technical Design Report for the ATLAS Inner Tracker Strip Detector, CERN-LHCC-2017-005, ATLAS-TDR-025, CERN, Geneva (2016), url : https ://cds.cern.ch/record/2257755 (cit. on p. 2).
5. G. Berruti, Radiation tolerant fiber optic humidity sensors for High Energy Physics Applications,PhD Thesis, Universita' degli Studi del Sannio CERN-THESIS-2015-32 (2015) 1 (cit. on p. 2).
6. ANSYS, ANSYS Fluent - CFD Software | ANSYS, 2016, url : http ://www.ansys.com/products/ fluids/ansys-fluent (cit. on p. 2).

Thank you for your attention